# Ratiometric Analysis of Single-Molecule Fluorescence Resonance Energy Transfer Using Logical Combinations of Threshold Criteria: A Study of 12-mer DNA

**Liming Ying, Mark I. Wallace, Shankar Balasubramanian,* and David Klenerman***

*The Department of Chemistry, University of Cambridge, Lensfield Road, Cambridge, CB2 1EW United Kingdom*

*Received: November 5, 1999; In Final Form: March 13, 2000*

Single-molecule fluorescence resonance energy transfer (FRET) combined with bulk fluorescence lifetimes, anisotropy, and spectra have been used to study a donor−acceptor labeled model DNA system (Cy5-5′-ACCTGCCGACGC-3′-TMR). A general ratiometric analysis method using independent donor and acceptor thresholding has been developed. Use of two logical combinations of thresholding criteria provides more information than either method alone, revealing heterogeneity within this system. Conditions yielding similar bulk fluorescence spectra can be readily distinguished by this single-molecule method. Fluorescence lifetimes and anisotropy measurements also suggest nonnegligible fluorophore−DNA interaction.

## Introduction

Recent advances in single-molecule spectroscopy and microscopy allow one to study the molecular properties and dynamic processes of biomolecules on an individual basis.[1−10] In contrast to conventional experiments, which measure ensemble averaged behavior, single-molecule measurements are able to probe the differences between individual molecules. The static heterogeneity and dynamic fluctuations in the conformations of DNA, protein, and other biological macromolecules demonstrate one such property that is difficult, if not impossible to detect at the bulk level, but can be potentially probed using single-molecule techniques.[11−16]

Fluorescence resonance energy transfer (FRET) is a widely used tool in biochemistry and structural biology.[17,18] In FRET, energy is nonradiatively transferred from an excited donor to an acceptor fluorophore with an efficiency that varies as the inverse sixth power of the distance between donor and acceptor. By attaching donor and acceptor dyes to two sites of a biomolecule, FRET can be used as a sensitive probe of intramolecular distance.

Recently, FRET has been introduced into the single-molecule regime.[4,15] Weiss and co-workers have established a ratiometric method to study subpopulations of single DNA molecules.[19,20] The fluctuations in energy transfer have been also used by several groups; for examples, studying the conformational dynamics of single SNase protein molecules during catalysis,[3] the ligand-induced conformational changes in single RNA three-way junctions,[9] and the folding dynamics of single GCN-4 peptides.[10]

Although single-molecule FRET has great potential as a tool for the investigation of biomolecular dynamics, care must be taken in attributing the change of FRET signal to the distance change between donor and acceptor. In single-molecule measurements, reasons for the fluctuation in energy transfer include: (1) reversible transitions to dark states;[6,21,22] (2) irreversible photobleaching;[1,15,23] (3) intersystem crossing to the triplet state;[24] (4) spectral diffusion;[25] (5) rotational dynamics of the dyes;[26,27] and (6) distance change between two dyes.[28] Therefore, it is essential to choose suitable control samples and examine both single-molecule and bulk measurements to fully understand the contributions from nondistance-change processes.

Well-defined sequences of DNA oligomers can now be routinely synthesized and labeled at specific sites with one or more fluorescent molecules. Consequently, FRET has been extensively applied in determining the structure and conformation of DNA molecules at an ensemble level.[29−35]

However, there is evidence to suggest that when many of these systems are examined in greater detail, a more complex picture emerges. For example, Clegg and co-workers have shown that for carboxytetramethylrhodamine (TMR) linked to DNA, multiple conformations exist with different quantum yields.[36] In addition, single-molecule lifetime measurements by Rigler et al. on TMR-labeled double-stranded DNA show fluctuation between two distinct conformations, one in which the TMR fluorophore is interacting with a guanine base and the other in which it is not.[37] Conformational fluctuations of single-TMR-labeled DNA molecules have also found to be nonergodic.[38−40] These results suggest that fluorescent heterogeneity may be an intrinsic property of dye-labeled DNA. Therefore, characterization of the fluorescence properties of dyes attached to DNA is important to ensure accurate interpretation of FRET data.

Motivated by these observations, we set out to assess the capabilities and limitations of single-molecule FRET in a study of DNA. A Cy5−12mer−TMR DNA system was chosen as a simple model. Changes in the FRET of single DNA molecules diffusing in solution were monitored, and a general method for identifying single-molecule FRET events has been developed. The single-molecule experiments are accompanied by bulk FRET, lifetime, and anisotropy measurements to justify the assumptions needed to perform the single-molecule analysis.

## Experimental Section

**Materials.** The 12-base oligonucleotides whose sequence is 5′-ACCTGCCGACGC-3′, with either carboxytetramethyl-

* To whom correspondence should be addressed. (E-mail: dk10012@cam.ac.uk and sb10031@cam.ac.uk).

10.1021/jp993914k CCC: $19.00 
Published on Web 05/03/2000

rhodamine (TMR) labeled at its 3′ end, or indodicarbocyanine (Cy5) labeled at its 5′ end or both, were purchased from Operon (Alameda, CA). A 13-mer complementary strand (5′-TGGACG-GCTGCGA-3′) was purchased from Oswel DNA Service (Southampton, UK). All oligonucleotides were HPLC purified. DNA duplexes were prepared by mixing 100 nM 12-mer and 10 $\mu$M 13-mer in 100 mM PBS buffer (pH = 7.4). Duplex samples were annealed by heating to 90 °C for 2 min and slowly cooling to room temperature (21 °C). Single-stranded samples (100 nM) were prepared in both 100 mM PBS buffer and MilliQ water.

**Steady-State Fluorescence Measurements.** Steady-state fluorescence spectra were measured on an Aminco-Bowman Series 2 Luminescence Spectrometer (Aminco, Urbana, IL). The excitation and emission band-passes were set to 4 nm. Next, 150-$\mu$L samples of labeled DNA at 100 nM concentration were excited at 515 nm and emission spectra were collected from 530 to 750 nm. All spectra were corrected for instrument response. Fluorescence anisotropies for donor (TMR) and acceptor (Cy5) were calculated from the polarization of the emission components $I_{VV}$, $I_{VH}$, $I_{HV}$, and $I_{HH}$ (where the subscripts denote the orientation of the excitation and emission polarizers) as $r = (I_{VV} - GI_{VH})/(I_{VV} + 2GI_{VH})$, where $G = I_{HV}/I_{HH}$. For TMR anisotropy, excitation was at 540 nm and emission spectra were collected at 580 nm; whereas for Cy5 anisotropy, the excitation wavelength was set to 630 nm and emission was measured at 670 nm. All measurements were performed at 21 °C.

**Time-Resolved Fluorescence Measurements.** Fluorescence lifetime measurements were made with the following apparatus. A frequency doubled, mode-locked Nd:YAG laser (Coherent Antares 76, 532 nm, 76 MHz, 70 ps) was used for both TMR excitation and to pump a dye laser (Coherent 702, DCM dye, 625 nm, 17 ps, 76 MHz) used to excite the Cy5 fluorophore. Both laser beams were attenuated with a combination of beam-splitters and neutral density filters. A 40-$\mu$W beam was directed into a modified inverted optical microscope (Diaphot 200, Nikon) using a dichroic mirror (540DRLP or 630DRLP, Omega) to focus 5 $\mu$m into the sample via the microscope objective (Fluor 100X, NA 1.30, Nikon). Emission was collected using the same objective, with a combination of dichroic, long-pass, and band-pass filters to reject scattered laser light. Fluorescence was detected with a fast photomultiplier (R4457, Hamamatsu). The pulses were processed using a time-correlated single photon counting card (SPC300, Edinburgh Instruments). This apparatus gave a full width at half maximum (fwhm) for the instrument response function of ~200 ps. The lifetime of TMR was measured at 100 nM concentration and that of Cy5 at 1 $\mu$M because of the lower photomultiplier efficiency at longer wavelengths. A sequence of four lifetime observations were made with the distance above the coverslip between 5 and 10 $\mu$m, these measurements were consistent within experimental error. In addition, focusing onto the coverslip results in a strong decrease in signal, indicating that contributions from DNA adsorbed on the glass surface can be neglected in our measurements.

**Single-Molecule FRET Measurements.** The apparatus used to achieve single-molecule detection is similar to that described previously.[41] The principal modification is in the dual-channel detection of the donor and acceptor fluorescence. A collimated laser beam (514.5 nm Argon ion, series 2000, Spectra Physics) was directed through a dichroic mirror and oil immersion objective (Fluor 100X, NA 1.30, Nikon) to focus 5 $\mu$m into a 20-$\mu$L sample solution supported on a cover glass. Fluorescence was collected by the same objective and imaged onto a 100-$\mu$m pinhole (Newport) to reject out of focus fluorescence and other background. Donor and acceptor fluorescence was then separated with a second dichroic mirror (630DRLP, Omega). Donor fluorescence was filtered by two band-pass filters (595RDF60 and 590DF35, Omega) before being focused onto an avalanche photodiode, APD (SPCM AQ-161, EG&G). Acceptor fluorescence was also filtered by long-pass and band-pass filters (565EFLP and 670DF40, Omega) before focusing onto a second APD (SPCM AQR-141, EG&G). Dark count rates for the two APDs were <50 counts/s. Outputs from the APDs were coupled to two PC implemented multichannel scalar cards (MCS−Plus, EG&G, Ortec), the synchronous start output of one MCS card being used to trigger the second. The time delay between two MCS cards was measured with a fast oscilloscope and found to be negligible. The overall detection efficiency of our apparatus is estimated at ~1%. Sample solutions of ~50 pM were used to achieve single-molecule FRET detection. To ensure stability of duplexed DNA at picomolar concentrations, 100-fold excess of the complementary strand was used to prepare a 100 nM sample, which was further diluted with a 10 $\mu$M PBS solution of the complementary strand just before measurement. This procedure results in a solution with a final duplex concentration of 50 pM. To ensure that we are observing genuine single-molecule FRET in the anticorrelation of photon bursts seen at single-molecule dilutions (Figure 4), control experiments were performed using single-labeled (TMR or Cy5) DNA under identical conditions.

**Ratiometric Method.** The following section describes the methods used to analyze the distribution of photon counts recorded by the two APDs.

The FRET efficiency $E$ is a function of the distance $R$ between donor and acceptor:

$$E = \frac{R_0^{\,6}}{R^6 + R_0^{\,6}} \tag{1}$$

where $R_0$ is the Förster distance at which 50% energy transfer occurs. The parameter $R_0$ is a function of orientation factor $\kappa^2$ and overlap intergral $J$.

$$R_0 = (8.79 \times 10^{-11}) n^{-4} \kappa^2 \Phi_d \langle J \rangle \tag{2}$$

where $\Phi_d$ is the quantum yield of donor and $n$ is the index of the medium. In single-molecule dual-channel detection, $E$ can be calculated by

$$E = \frac{I_a}{I_a + \dfrac{\Phi_a \eta_a}{\Phi_d \eta_d} I_d} \tag{3}$$

where $I_a$ describes the number of photons detected in the acceptor channel for a particular time bin and $I_d$ is the corresponding signal in the donor channel; $\Phi_d$ and $\Phi_a$ denote the quantum yields for donor and acceptor, respectively; and $\eta_d$ and $\eta_a$ are collection efficiencies for donor and acceptor channels, respectively.

To ensure that changes in FRET efficiency are dominated by distance-changes, it is important that $R_0$, and hence $\kappa^2$, can be assumed to be constant. In addition, to directly obtain the single-molecule FRET efficiency, the ratio of quantum yields in eq 3 must also be assumed constant. Fluorescence lifetime measurements by Rigler and co-workers[37] show two discrete lifetimes at the single-molecule level, which suggests that a

distribution of quantum yields is likely to be present. Rather than make the assumption that each molecule has an identical quantum yield, we chose to examine the proximity ratio $P$.

$$P = \frac{I_a}{I_a + I_d} \tag{4}$$

The parameter $P$ differs from the FRET efficiency $E$ by the absence of a term describing the quantum yields of donor and acceptor and collection efficiencies for both channels. As such, any fluctuation in quantum yield will be reflected in the proximity ratio distribution.

Although $P$ cannot be linked directly to interfluorophore distance, it is still a good indicator of fluorophore separation.[9] This ratiometric approach was first suggested by Weiss and coworkers,[20] and was described more recently by the same group.[19]

For complete rapid randomization of the relative orientations between donor and acceptor, the orientational factor $\kappa^2$ has a constant value of 2/3.[42] However, it should be noted that for $\kappa^2$ to be 2/3, it is not necessary that the condition of dynamically rapid averaging hold. This value is possible even between two absolutely rigid dipoles.[42,43] A $\kappa^2$ value of 2/3 is a good approximation for many cases of only partial orientational freedom.[42,44,45] In these experiments, the fluorescence anisotropy of the TMR fluorophore is low $<0.1$ in all the dual-labeled DNA studied. It is therefore assumed that the orientation factor is constant in our proximity ratio analysis. Any fluctuation in fluorophore orientation will result in broadening of the proximity ratio distribution.

The signals $I_a$ and $I_d$ have a number of sources; these are, photon counts from fluorescent molecules ($m_a$ and $m_d$), background counts ($b_a$ and $b_d$), and cross-talk between the two detection channels ($\alpha_a$ and $\alpha_d$)

$$I_a = m_a + b_a + \alpha_a I_d \tag{5}$$

$$I_d = m_d + b_d + \alpha_d I_a \tag{6}$$

The primary sources of background signal arise from scattered light and out of focus fluorescence. These effects can be estimated by collecting data from samples of the pure solvent and fitting the donor and acceptor channel counts to Poisson distributions with mean values $\beta_a$ and $\beta_d$. The cross-talk parameters, $\alpha_a$ and $\alpha_d$, may also be estimated by calculating the mean ratio of acceptor-to-donor intensity for single-labeled TMR−DNA, and equivalently, the ratio of donor-to-acceptor intensity for single-labeled Cy5−DNA. For this apparatus, a value of ~6.3% for $\alpha_a$ was obtained, whereas $\alpha_d$ is negligibly small ($<0.5\%$). This value is consistent with a cross-talk estimate based on the expected transmission of the emission spectrum of single-labeled TMR−DNA through dichroic and band-pass filters.

After subtraction of the mean backgrounds and correction for cross-talk, the calculated proximity ratio becomes:

$$P = \frac{I_a - \beta_a - \alpha_a I_d}{(I_a - \beta_a - \alpha_a I_d) + (I_d - \beta_d)} \tag{7}$$

The only minor factor not incorporated in this treatment is the effect of direct Cy5 excitation. Inclusion of direct excitation would lead to a fixed shift in the observed acceptor signal by ~2% of the donor photon counts.

Before the proximity ratio can be calculated, the raw data must be thresholded to reject signals not due to FRET. Great care must be taken in choosing the thresholding algorithm to optimize the information extracted from the data. Digital communication theory[46] provides a mathematical framework within which optimal threshold values can be calculated.

In the simplest approximation to the experimental conditions, both the molecular signal $m$ and the background $b$ are randomly distributed. Given the probability $P_f$ that the probe volume contains a fluorophore, the mean molecular signal $\mu$, and the mean background $\beta$, the decision threshold $T$ is given by:[46]

$$T = \frac{\ln\left(\frac{1 - P_f}{P_f}\right) + \mu}{\ln\left(\frac{\beta + \mu}{\beta}\right)} \tag{8}$$

From estimates of $\mu$ and $P_f$, discrete threshold values for donor and acceptor channels are estimated to be ~6 for donor and ~4 for the acceptor channel.

There are two logical alternatives by which the thresholding criteria for the two channels may be combined; these are, to accept only those signals where both donor *AND* acceptor are above their threshold values, or to accept only those signals where either donor *OR* acceptor are greater than their thresholds. The first scheme (*AND*) will select only those FRET signals that are distinguishable above the distribution of background noise in *both* channels. This scheme ensures that the distribution of proximity ratios formed from this population will be dominated by changes due to FRET. However, this scheme does reject those FRET signals for which the molecular signal (in either channel) has become indistinguishable from the background. For this experiment, the *AND* method describes a subset of all the FRET events and will not represent the true proximity distribution for low ($<0.20$) or high ($>0.80$) values of $P$.

The second scheme (*OR*) includes data for which the molecular signal in one channel is below the threshold. In this way, the presence of any very low or very high proximity components to the distribution can be detected. However, in this case, the components from which the proximity ratio distribution is formed (the donor and acceptor photon counts) now combine both background and FRET distributions. However, even these signals only come from events where one of the two components exhibits signal greater than the background-rejecting threshold:

for low P, the distribution will be dominated by the background signal in the acceptor channel, for the cases where high donor counts are observed;

for high P, the distribution will be dominated by the background signal in the donor channel, for the cases where high acceptor counts are observed.

However, as the number of bursts due to FRET events are many times greater than the number of bursts due to impurities (seen from control experiments described in the single-molecule results section), the presence of a signal in the *OR* distribution indicates that a FRET event has occurred. Assuming that the background signal is constant (as confirmed by the same control experiments), changes in the magnitude of general features of this distribution indicate changes in FRET. Use of these two methods in conjunction provides greater insight into the distribution of interfluorophore separation than by application of either method alone.

The random fluctuations in signal due to photon shot-noise results in uncertainty in the true value of the proximity ratio, which can be estimated using a standard analysis of error: Variables $I_a$ and $I_d$ have random fluctuations ($\Delta I_a =$

$\sqrt{\xi_a}$, $\Delta I_d = \sqrt{\xi_d}$) about their mean values $\xi_a$ and $\xi_d$ due to intensity shot-noise. The standard deviation of ratio $P$ can be calculated by

$$(\Delta P)^2 = \left(\frac{\partial P}{\partial I_a}(I_a = \xi_a, I_d = \xi_d)\Delta I_a\right)^2 + \left(\frac{\partial P}{\partial I_d}(I_a = \xi_a, I_d = \xi_d)\Delta I_d\right)^2$$

$$= \frac{\xi_d^{\,2}}{(\xi_a + \xi_d)^4}\Delta I_a^{\,2} + \frac{\xi_a^{\,2}}{(\xi_a + \xi_d)^4}\Delta I_d^{\,2}$$

$$= \frac{\xi_a \xi_d^{\,2}}{(\xi_a + \xi_d)^4} + \frac{\xi_a^{\,2}\xi_d}{(\xi_a + \xi_d)^4}$$

$$= \frac{\xi_a \xi_d}{(\xi_a + \xi_d)^3} \tag{9}$$

Introducing

$$\gamma = \frac{\xi_a}{\xi_d + \xi_a} \tag{10}$$

and for a particular fixed threshold $T$

$$\Delta P(\xi_d = T_d) = \left(\frac{\gamma}{T_d}\right)^{1/2}(1 - \gamma) \tag{11}$$

or

$$\Delta P(\xi_a = T_a) = \left(\frac{1 - \gamma}{T_a}\right)^{1/2}\gamma \tag{12}$$

Selecting the *AND* thresholding criteria, the uncertainty boundary can be estimated by

$$\Delta P(\xi_a = T_a \cap \xi_d = T_d) = \left(\frac{\gamma(1 - \gamma)^2}{T_d} + \frac{\gamma^2(1 - \gamma)}{T_a}\right)^{1/2} \tag{13}$$

Likewise, if we select an *OR* thresholding criteria,

$$\Delta P(\xi_a = T_a \cup \xi_d = T_d) = \begin{cases} \left(\frac{\gamma}{T_d}\right)^{1/2}(1-\gamma) & 0 \le \gamma \le 0.5 \\ \left(\frac{1-\gamma}{T_a}\right)^{1/2}\gamma & 0.5 \le \gamma \le 1 \end{cases} \tag{14}$$

Figure 1 presents the results of this analysis using the thresholds applied in the single-molecule experiment (details in next section).

If the detected signals do not contain information regarding the heterogeneity of the DNA sample, but just reflect the shot-noise, their distributions can be described by two independent Poisson variables. We can model these distributions to compare the statistically random case with our experimental results, which helps to illuminate the effects of thresholding on our data. Mean values of donor and acceptor intensities were extracted from experimental data using *OR* thresholding (donor > 7 counts per bin or acceptor > 7 counts per bin). Integer values ($\mu_a = 4$, $\mu_d = 14$) were then selected for the simulation based on these means. The proximity ratio distribution was simulated for signals from 0 to 150 counts (i.e., 99.99% of all experimental signals) and results are shown in Figure 2. The corrugations seen on the leading edge of the un-binned distributions are due to the discrete nature of the counting events. Once suitably binned, these distributions can be well described by a beta function.[19] The *OR* thresholding has little effect on the simulated proximity ratio distribution. Applying *AND* thresholding to the simulation confirms that only a relatively small subset of FRET events is selected.

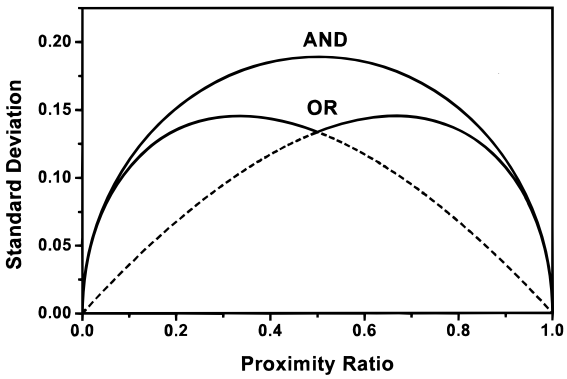


**Figure 1.** Estimate of the uncertainty in proximity ratio due to the thresholding criteria. Solid lines correspond to the two different criteria: upper curve, *AND* (eq 13); lower curve, *OR* (eq 14). Dotted lines represent the two components of the *OR* condition.

**TABLE 1: Fluorescence Anisotropy of TMR and Cy5 Bound to DNA**

| sample | solvent | Cy5 anisotropy | TMR anisotropy |
|---|---|---|---|
| ss-DNA−TMR | $H_2O$ | − | $0.062 \pm 0.002$ |
| ss-DNA−TMR | PBS | − | $0.108 \pm 0.002$ |
| ds-DNA−TMR | PBS | − | $0.159 \pm 0.003$ |
| Cy5−ss-DNA | $H_2O$ | $0.092 \pm 0.005$ | − |
| Cy5−ss-DNA | PBS | $0.196 \pm 0.003$ | − |
| Cy5−ds-DNA | PBS | $0.254 \pm 0.006$ | − |
| Cy5−ss-DNA−TMR | $H_2O$ | $0.202 \pm 0.010$ | $0.047 \pm 0.002$ |
| Cy5−ss-DNA−TMR | PBS | $0.112 \pm 0.002$ | $0.066 \pm 0.004$ |
| Cy5−ds-DNA−TMR | PBS | $0.231 \pm 0.010$ | $0.096 \pm 0.002$ |

This simulation highlights the effect of thresholding on our data and predicts the general shape of distributions we would expect if the distribution of fluorescence signal is dominated by shot-noise. In this way, it provides a reference distribution to which the experimental distribution can be compared. In the *Results* section we show that the observed distribution is quite different from this reference distribution and that this difference is most likely due to molecular heterogeneity.

## Results

**Steady-State Fluorescence.** Steady-state fluorescence and anisotropy measurements were taken for all the samples described in this paper. Figure 3 depicts the fluorescence spectrum of single- and double-stranded Cy5−12mer−TMR under different conditions. The reference spectra were generated from the sum of the two single-labeled (TMR or Cy5) samples under 515 nm excitation, 100 nM concentration, and normalized to the peak of the TMR fluorescence. A 4-nm red shift of TMR fluorescence is observed for all double-labeled DNA relative to the equivalent single-labeled DNA spectra. The significant Cy5 emission, above the level due to direct excitation and cross-talk, shows strong evidence for FRET, albeit the efficiency is low ($P \approx 0.18$). It is also worth noting that it is difficult to distinguish between the three different systems from this bulk measurement.

Fluorescence anisotropy measurements (Table 1) show that TMR−DNA may be regarded as a free rotor, except for the case of single-labeled ds-DNA in PBS buffer, where the anisotropy is surprisingly high ($0.159 \pm 0.003$), possibly due to interaction with the DNA. These results are in agreement

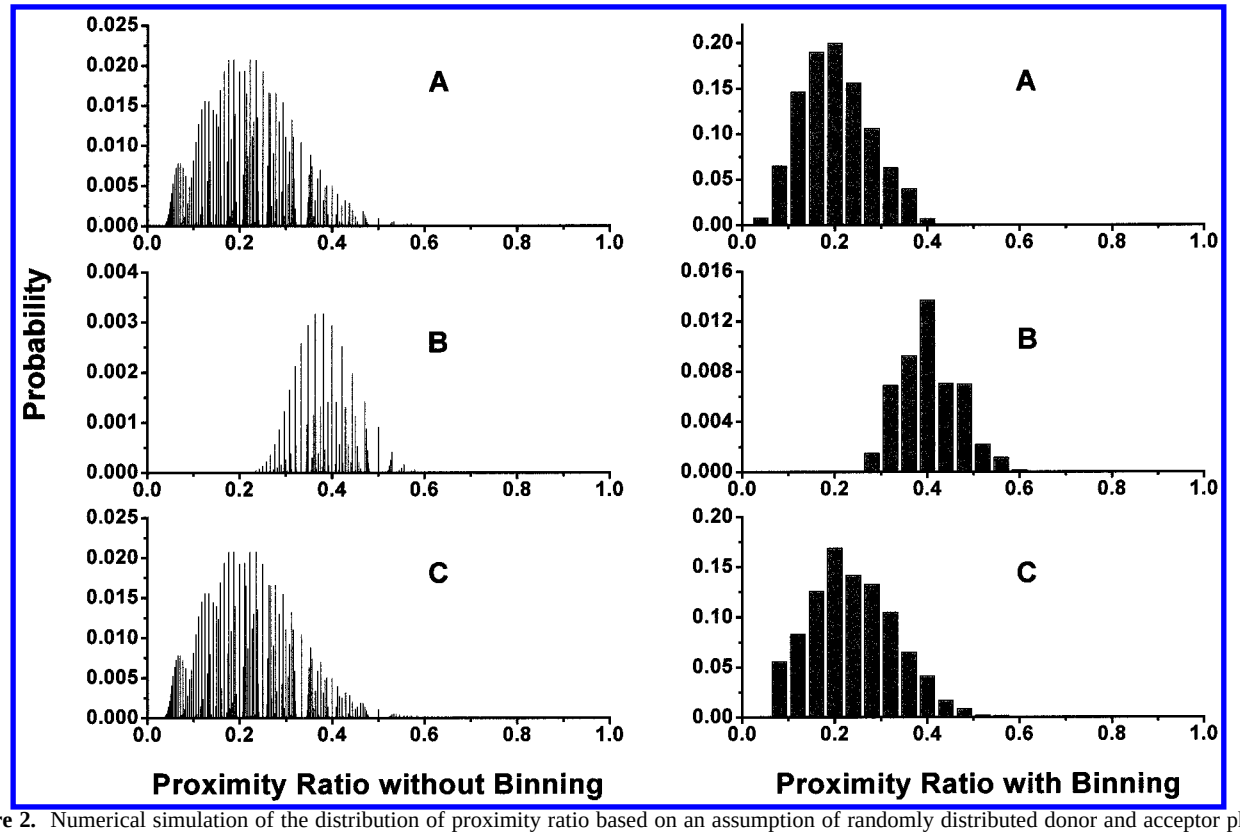


**Figure 2.** Numerical simulation of the distribution of proximity ratio based on an assumption of randomly distributed donor and acceptor photon bursts, with means $m_d = 14$ and $m_a = 4$: (A) no thresholding criteria; (B) *AND* thresholding; and (C) *OR* thresholding.

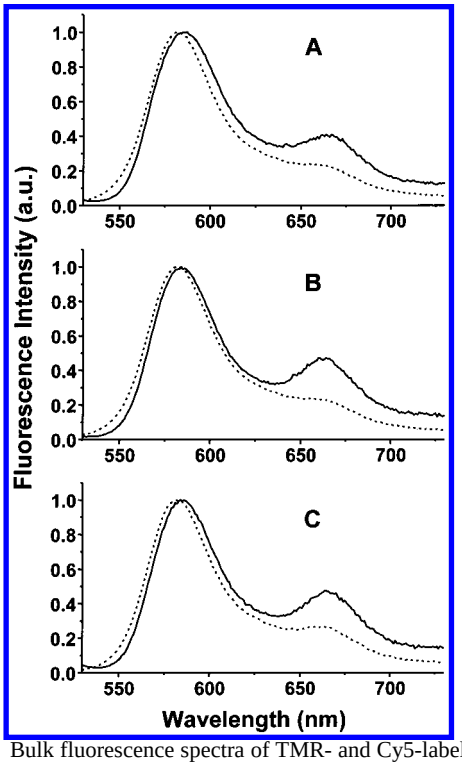


**Figure 3.** Bulk fluorescence spectra of TMR- and Cy5-labeled DNA. In all cases, 515 nm excitation and 100 nM concentration were used. Spectra were corrected for instrument response and normalized to TMR fluorescence (≈580 nm). Solid lines correspond to double-labeled DNA, and dotted lines represent the sum of emission spectra from single-labeled (TMR and Cy5) 12-mers: (A) ss-12-mer in PBS buffer; (B) ds-12-mer/13-mer in PBS buffer; and (C) ss-12-mer in MilliQ water. Significant Cy5 emission in all three spectra provides evidence for FRET.

with previous experiments.[36] The anisotropy of Cy5 is larger than TMR, except in the cases of single-labeled ss-DNA in MilliQ water and double-labeled ss-DNA in PBS buffer. The anisotropy of all fluorophores increases on addition of the complementary strand to the sample.

**Time-Resolved Fluorescence.** The isotropic fluorescence decay curves were analyzed by deconvolution of instrument response with a multiexponential model. The quality of fit was judged by reduced $\chi^2$. This procedure results in all curves being adequately described by double exponential decay, except for the case of single-labeled ds-TMR−DNA, where a third very short-lifetime component (0.147 ± 0.012 ns) is required. The presence of a third short-lifetime component is consistent with the dark state reported by Clegg and co-workers.[36] These results (Tables 2 and 3) show TMR to be ∼90% single-exponential, whereas Cy5 exhibits significant biexponential decay.

In going from MilliQ to PBS buffer, all lifetimes are shortened; possible explanations for this result include ionic interaction between solvent and dye, dye−DNA interaction, or changes in lifetime as a result of altered DNA conformation. Also of interest are the changes in going from single- to double-labeled samples in PBS: $<\tau>$ of TMR−DNA increases and $<\tau>$ for Cy5−ss-DNA decreases. The final point of note is the 14% increase in $\tau_1$ for TMR−DNA on addition of an excess of complimentary strand to double-labeled DNA. This increase is most likely due to the increase in relative distance between the two fluorophores, which is due to increased stiffness of double-stranded DNA compared with the single-stranded DNA. Another possibility is that there is less rotational freedom of TMR in ds-DNA, therefore less dynamic quenching by DNA bases.

**Single-Molecule FRET.** Figure 4A is an example of a 0.5-ms integration time, two-channel photo burst trajectory for a 50 pM DNA solution excited at 514.5 nm. Most bins are occupied by the background signal, but anticorrelated photon bursts can be clearly seen in the expanded panel (Figure 4B). The signal from direct excitation of Cy5 is estimated to be ∼2%

**TABLE 2: Fluorescence Lifetimes of TMR Bound to DNA[a]**

| sample | solvent | $\tau_1$ (ns) | % $\tau_1$ | $\tau_2$ (ns) | % $\tau_2$ | $<\tau>$ (ns) | $\chi^2$ |
|---|---|---|---|---|---|---|---|
| ss-DNA−TMR | $H_2O$ | 2.758 ± 0.013 | 90.1 | 0.497 ± 0.008 | 9.9 | 2.535 | 1.254 |
| ss-DNA−TMR | PBS | 2.637 ± 0.013 | 88.2 | 0.506 ± 0.007 | 11.8 | 2.356 | 1.242 |
| ds-DNA-TMR | PBS | 2.440 ± 0.027 | 81.5 | 0.673 ± 0.018 | 18.5 | 2.113 | 1.647[b] |
| Cy5−ss-DNA−TMR | $H_2O$ | 3.371 ± 0.015 | 97.1 | 0.451 ± 0.017 | 2.9 | 3.290 | 1.341 |
| Cy5−ss-DNA−TMR | PBS | 2.587 ± 0.020 | 96.5 | 0.444 ± 0.023 | 3.5 | 2.512 | 1.136 |
| Cy5−ds-DNA−TMR | PBS | 3.003 ± 0.018 | 91.7 | 0.422 ± 0.009 | 8.3 | 2.789 | 1.157 |

[a] ss-DNA indicates the sequence 5′-ACCTGCCGACGC-3′; ds-DNA represents this sequence hybridized to 5′-TGGACGGCTGCGA-3′. [b] Fitting to three exponentials gives $\tau_1 = 3.211 \pm 0.035$ (61.3%), $\tau_2 = 1.132 \pm 0.024$ (32.7%), $\tau_3 = 0.147 \pm 0.012$ (5.9%), $<\tau> = 2.347$, and $\chi^2 = 1.188$.

**TABLE 3. Fluorescence Lifetimes of Cy5[a]**

| sample | solvent | $\tau_1$ (ns) | % $\tau_1$ | $\tau_2$ (ns) | % $\tau_2$ | $<\tau>$ (ns) | $\chi^2$ |
|---|---|---|---|---|---|---|---|
| Cy5−ss-DNA | $H_2O$ | 1.736 ± 0.022 | 79.4 | 0.844 ± 0.038 | 20.6 | 1.552 | 1.072 |
| Cy5−ss-DNA | PBS | 1.751 ± 0.026 | 75.6 | 0.872 ± 0.037 | 24.4 | 1.537 | 1.067 |
| Cy5−ds-DNA | PBS | 1.376 ± 0.006 | 83.5 | 0.625 ± 0.027 | 16.5 | 1.252 | 1.014 |
| Cy5−ss-DNA−TMR | $H_2O$ | 1.733 ± 0.036 | 75.6 | 0.818 ± 0.050 | 24.4 | 1.510 | 1.004 |
| Cy5−ss-DNA−TMR | PBS | 1.605 ± 0.030 | 75.9 | 0.757 ± 0.047 | 24.1 | 1.401 | 1.009 |
| Cy5−ds-DNA−TMR | PBS | 1.552 ± 0.032 | 72.4 | 0.842 ± 0.046 | 27.6 | 1.356 | 1.048 |

[a] ss-DNA indicates the sequence 5′-ACCTGCCGACGC-3′, ds-DNA represents this sequence hybridized to 5′-TGGACGGCTGCGA-3′.

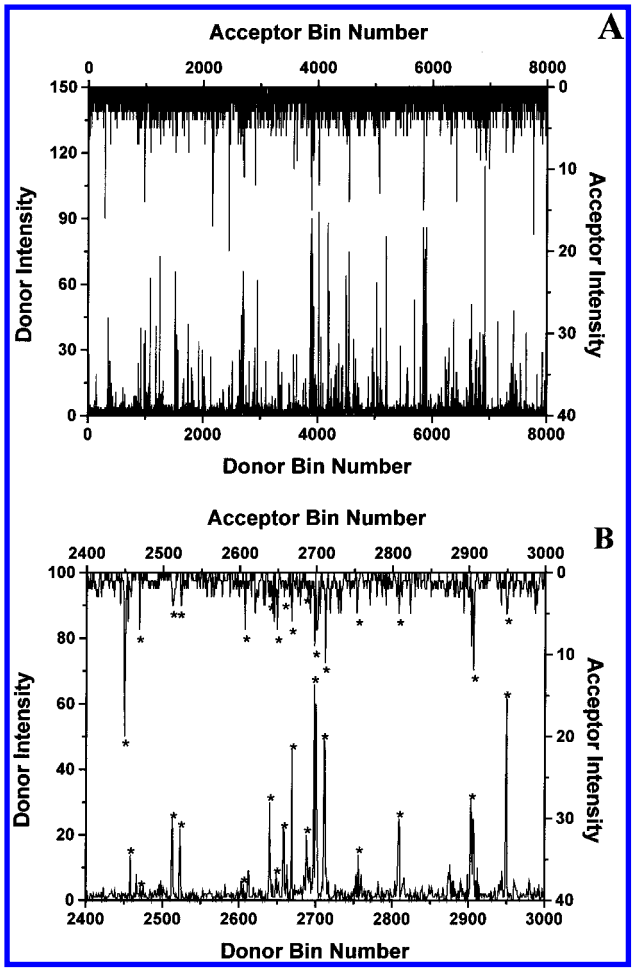


**Figure 4.** (A) Two-channel photon burst trajectory for a 50-pM solution of double-labeled ss-DNA diffusing in MilliQ water. Each bin corresponds to an integration time of 0.5 ms. Excitation power is 0.2 mW at 514.5 nm. (B) An expanded view of a section of Figure 4A. Anticorrelated photon bursts from donor and acceptor channels are clearly visible as indicated by ∗.

of the TMR signal based on bulk absorption and fluorescence spectra measurements of Cy5-labeled DNA. Control experiments on single-labeled ss-DNA with a single TMR or Cy5 label show no anticorrelation of signal. The only mechanism capable of producing strongly anticorrelated photon burst is FRET. Cross-talk from donor to acceptor was calculated from the photon burst trajectory of single-labeled TMR−ss-DNA and was subtracted in the proximity ratio. Mean values of the donor and acceptor background levels were measured using PBS and MilliQ solutions without the addition of fluorescently labeled DNA, giving values of 0.6 and 0.9 counts, respectively. Thresholding criteria were determined by examination of the background signal distribution. A threshold of 7 counts for either donor or acceptor channels ensures that 99.9% of the selected burst events will be from the fluorophore of interest. As expected, this value is slightly larger than the theoretical minima ($I_d \geq 6$ and $I_a \geq 4$) estimated with eq 6.

Figure 5 depicts the distribution of proximity ratio as defined in eq 5 for single-molecule double-labeled DNA (*AND* thresholding corresponds to the left-hand set of histograms and *OR* thresholding is shown on the right). Note that the number of *AND* events is much lower than the number of *OR* events as would be expected for our relatively low FRET system. The proximity ratio distributions are quite different from the simulation in Figure 2, suggesting that a distribution of molecular states must be present. Use of the *AND* selection rule, which selects the subset of FRET events that can be truly separated from the background, enables the ds-DNA to be resolved from the single-stranded samples. The *OR* selection rule, which selects most of the FRET events, permits ss-DNA in MilliQ to be distinguished from the samples in PBS buffer by the presence of a high proximity ratio component (Figure 5, bottom right histogram).

## Discussion

During the last 5 years, conformational heterogeneity has been reported for both bulk and single-molecule TMR−DNA.[36,37] In these experiments, heterogeneity is attributed to the changing local environment of the TMR fluorophore. In particular, a quenching mechanism due to electron transfer to guanine residues in the DNA chain is suggested. Our results for TMR−DNA show a second weak lifetime component that may also be attributed to this quenching mechanism.

Anisotropy results show that the TMR fluorophore is more mobile than Cy5 and on introduction of Cy5, TMR anisotropy decreases. This result suggests that the Cy5 fluorophore could affect the conformation of DNA, which may partially account for the increase of donor lifetime observed in our model system. These experimental observations indicate that great care must be taken in interpreting any DNA FRET measurement based

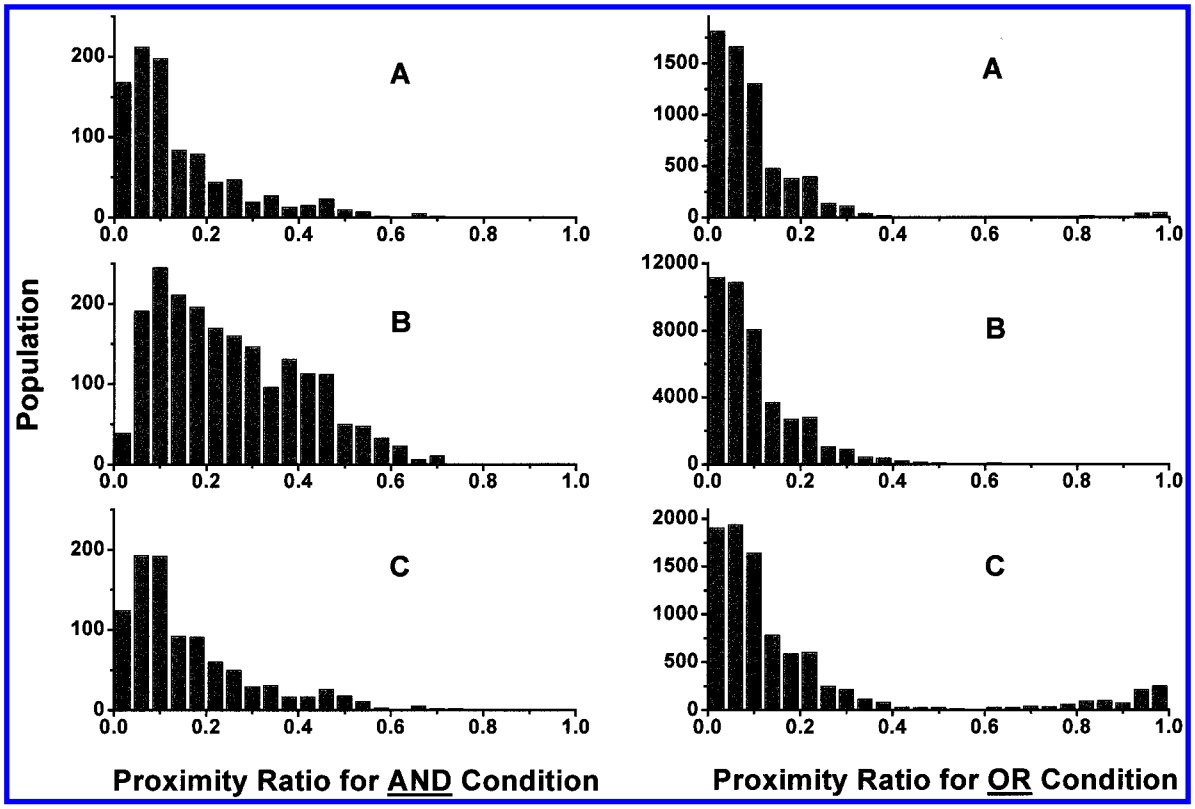


**Figure 5.** Single-molecule proximity ratio distribution determined using *AND* and *OR* thresholding criteria. Background and cross-talk were subtracted. (A) ss-DNA in PBS buffer, (B) ds-DNA in PBS buffer; and (C) ss-DNA in MilliQ water. All three samples show a low proximity ratio. Also of note is the high FRET component appearing in sample (C). Only through the use of both thresholding criteria can the different conformations of DNA present in the three systems be distinguished.

solely on donor fluorescence quenching or the increase in acceptor fluorescence.

It can be seen from the differences between the observed proximity ratio distributions and our simulation (in that we cannot accurately describe the experimental distributions with the beta function present in the simulation), that shot-noise cannot be the only component present. All the double-labeled DNA samples show a small TMR anisotropy and medium Cy5 anisotropy, suggesting that changes in the distance between the fluorophores rather than the orientation factor is the main contribution to the fluctuations in the proximity ratio. Assuming that the distribution of fluorescence quantum yields is not dominant (as indicated by the small changes in bulk fluorescence lifetimes), our results suggest DNA conformational heterogeneity exists in this system.

Single-molecule measurements of double-labeled ss-DNA in water show a conformational component (10%) with very low donor and higher acceptor fluorescence that is only discovered using the *OR* criteria. This component cannot be detected in our measurements of bulk fluorescence or using the *AND* criteria alone, which shows the advantage of doing single-molecule analysis using both *AND* and *OR* criteria. The higher FRET component may correspond to a structure with the donor and acceptor in close proximity. Possible explanations for this component include the effects of fluorophore linkers or the presence of a bent DNA structure bringing the two fluorophores close together. This result highlights the usefulness of a single-molecule ratiometric method in understanding DNA conformation.

Given that our single-molecule FRET results appear to be dominated by the distance separation between the two fluorophores, comparisons can be made with other experiments that describe the conformation of DNA in solution. Direct measurements of the persistence length of DNA have been made recently.[47−50] Atomic force microscopy experiments reported a persistence length of 53 nm for ds-DNA.[47] In contrast, ss-DNA shows much shorter persistence lengths. For instance, Smith et al. used laser tweezers to obtain a value of 0.75 nm for mixed-sequence (bacteriophage lamda) ss-DNA,[48] whereas Mills et al. performed transient electric birefringence measurements to derive a value of 2−3 nm.[50] Our observation of a high proximity ratio component of ss-DNA in water is also consistent with the short persistence length of ss-DNA. The wormlike chain model (WLC) has also been shown to provide an appropriate description of the elastic behavior of DNA.[49] The WLC model relates mean-square end-to-end distance $\langle R^2 \rangle$, persistence length $P_l$, and contour length $L$ as follows,

$$\langle R^2 \rangle = 2PL\left(1 - \frac{P_1}{L}(1 - e^{-L/P})\right) \qquad (15)$$

With these statistical results in mind, it is not difficult to rationalize the small apparent difference between the bulk fluorescence spectra of single- and double-stranded DNA. Assuming a helix pitch of 0.34 nm for the DNA duplex, the expected end-to-end distance for a 12-base pair ds-DNA is 4.1 nm. For ss-DNA, assuming an internucleotide distance of 0.6 nm, we arrive at a contour length of ∼7.2 nm. Estimating the persistence length of our sample at 2 nm, the root mean square (rms) end-to-end length is ∼4.6 nm based on the WLC model. These results suggest that, neglecting any change in fluorophore, ensemble-averaged fluorescence spectra for ss- and ds-DNA should be very similar, a conclusion supported by our bulk fluorescence spectra. Based on the transmission curves of the filters used, we estimate bulk fluorescence to yield mean proximity ratios of 0.17 for ss-DNA and 0.19 for ds-DNA.

Experimentally, we observe identical mean proximity ratios for the *OR* criteria for the ss-DNA and ds-DNA (0.11), which is similar but not identical to the bulk results. However, the ratios are quite different for the *AND* criteria (0.14 for ss-DNA, 0.25 for ds-DNA). The *OR* criteria select almost all FRET events so should, as observed, give agreement with the bulk results. The *AND* combination of thresholding, in contrast, only selects a *subset* of FRET events where the donor and acceptor emission are both strong. The fraction of the total population selected will depend on the level of FRET in the system. In the case of the ds-DNA, this fraction is only 5% of the total events. Therefore, it is not surprising that different selection criteria should give different values for the mean proximity ratio. The difference between bulk and the *OR* criteria in single-molecule proximity ratio may also be expected because

$$\frac{\langle I_a \rangle}{\langle I_a \rangle + \langle I_d \rangle} \neq \left\langle \frac{I_a}{I_a + I_d} \right\rangle \tag{16}$$

In addition, the single molecule experiments are only performed on the subset of all molecules that is sufficiently bright to be detected. Dim or dark molecules may intrinsically exist, which could also explain the difference between the bulk and single molecule proximity ratios in the case of *OR* thresholding.

We have shown that despite the great difficulty in determining exact single-molecule FRET distances, conformational heterogeneity can still be examined. For the 12-mer DNA we studied, we have shown that in water there is a subset of the population with a high proximity ratio. In addition, this experiment also suggests that if quantitative distance measurements are required from a single-molecule FRET experiment, single-molecule fluorescence lifetime and orientation should also be measured. These results have demonstrated some of the potentials and limitations of single-molecule FRET as a tool for increasing our understanding of the secondary structure of nucleic acids.

## Conclusions

We have presented a general method to analyze single-molecule FRET intensities using a ratiometric method and well-justified thresholding criteria. The use of both *AND* and *OR* criteria provides greater information than the use of either criteria alone. We have applied this method to a dual-labeled 12-mer DNA, that shows low bulk FRET to reveal conformational heterogeneity. Only through the use of combinations of two independent thresholding parameters of both donor and acceptor intensities can we distinguish single-stranded and double-stranded DNA in MilliQ and PBS buffer. The fluorescence lifetimes and anisotropy measurements indicate a nonnegligible fluorophore−DNA interaction.

**Acknowledgment.** We acknowledge the help of Colin Barnes for his advice on the handling and design of the DNA sequences. We also thank the reviewers of the paper for constructive suggestions and criticisms. This work was supported by the Leverhulme Trust (Grant #F65OE).

## References and Notes

(1) Xie, X. S.; Trautman, J. K. *Annu. Rev. Phys. Chem*. **1998**, *49*, 441.
(2) Nie, S. M.; Zare, R. N. *Annu. Rev. Biophys. Biomol. Struct*. **1997**, *26*, 567.
(3) Ha, T.; Ting, A. Y.; Liang, J.; Caldwell, W. B.; Deniz, A. A.; Chemla, D. S.; Schultz, P. G.; Weiss, S. *Proc. Natl. Acad. Sci. U.S.A.* **1999**, *96*, 893.
(4) Weiss, S. *Science* **1999**, *283*, 1676.
(5) Lu, H. P.; Xun, L.; Xie, X. S. *Science* **1998**, *282*, 1877.
(6) Dickson, R. M.; Cubitt, A. B.; Tien, R. Y.; Moerner, W. E. *Nature* **1997**, *388*, 355.
(7) Vale, R. D.; Funatsu, T.; Pierce, D. W.; Romberg, L.; Harada, Y.; Yanagida, T. *Nature* **1996**, *380*, 451.
(8) Ying, L.; Xie, X. S. *J. Phys. Chem. B* **1998**, *102*, 10399.
(9) Ha, T.; Zhuang, X.; Kim, H. D.; Orr, J. W.; Williamson, J. R.; Chu, S. *Proc. Natl. Acad. Sci. U.S.A.* **1999**, *96*, 9077.
(10) Jia, Y.; Talaga, D. S.; Lau, W. L.; Lu, H. S. M.; DeGrado, W. F.; Hochstrasser, R. M. *Chem. Phys.* **1999**, *247*, 69.
(11) Bartko, A. P.; Dickson, R. M. *J. Phys. Chem. B* **1999**, *103*, 11237.
(12) Higgins, D. A. *J. Phys. Chem. B* **1998**, *102*, 7231.
(13) Dunn, R. C.; Talley, C. E. *J. Phys. Chem. B* **1999**, *103*, 10214.
(14) Empedocles, S. A.; Neuhauser, R.; Bawendi, M. G. *Nature* **1999**, *399*, 126.
(15) Ha, T.; Enderle, T.; Ogletree, D. F.; Chemla, D. S.; Selvin, P. R.; Weiss, S. *Proc. Natl. Acad. Sci. U.S.A.* **1996**, *93*, 6264.
(16) Ruiter, A. G. T.; Veerman, J. A.; Garcia Parajo, M. F.; van Hulst, N. F. *J. Phys. Chem. A* **1997**, *101*, 7318.
(17) Clegg, R. M. *Methods Enzymol*. **1992**, *211*, 353.
(18) Selvin, P. R. *Methods Enzymol*. **1995**, *246*, 300.
(19) Dahan, M.; Deniz, A. A.; Ha, T.; Chemla, D. S.; Schultz, P. G.; Weiss, S. *Chem. Phys*. **1999**, *247*, 85.
(20) Deniz, A. A.; Dahan, M.; Grunwell, J. R.; Ha, T.; Faulhaber, A. E.; Chemla, D. S.; Weiss, S.; Schultz, P. G. *Proc. Natl. Acad. Sci. U.S.A.* **1999**, *96*, 3670.
(21) Bopp, M. A.; Jia, Y.; Li, L.; Cogdell, R. J.; Hochstrasser, R. M. *Proc. Natl. Acad. Sci. U.S.A.* **1997**, *94*, 10630.
(22) Vanderbout, D. A.; Yip, W. T.; Hu, D.; Fu, D. K.; Swager, T. M.; Barbara, P. F. *Science* **1997**, *277*, 1074.
(23) Sanchez, E. J.; Novotny, L.; Holtom, G. R.; Xie, X. S. *J. Phys. Chem. A* **1997**, 7019.
(24) Veerman, J. A.; Garcia Parajo, M. F.; Kuipers, L.; van Hulst, N. F. *Phys. Rev. Lett.* **1999**, *83*, 2155.
(25) Lu, H. P.; Xie, X. S. *Nature* **1997**, *385*, 143.
(26) Ha, T.; Enderle, T.; Chemla, D. S.; Selvin, P. R.; Weiss, S. *Phys. Rev. Lett.* **1996**, *77*, 3979.
(27) Ha, T.; Glass, J.; Enderle, T.; Chemla, D. S.; Weiss, S. *Phys. Rev. Lett.* **1998**, *80*, 2093.
(28) Ha, T.; Ting, A. Y.; Liang, J.; Deniz, A. A.; Chemla, D. S.; Schultz, P. G.; Weiss, S. *Chem. Phys*. **1999**, *247*, 107.
(29) Clegg, R. M.; Murchie, A. I. H.; Zechel, A.; Lilley, D. M. J. *Proc. Natl. Acad. Sci. U.S.A.* **1993**, *90*, 2994.
(30) Furey, W. S.; Joyce, C. M.; Osborne, M. A.; Klenerman, D.; Peliska, J. A.; Balasubramanian, S. *Biochemistry* **1998**, *37*, 2979.
(31) Tóth, K.; Sauermann, V.; Langowski, J. *Biochemistry* **1998**, *37*, 8173.
(32) Ota, N.; Hirano, K.; Warashina, M.; Andrus, A.; Mullah, B.; Hatanaka, K,; Taira, K. *Nucleic Acid Res*. **1998**, *26*, 735.
(33) Simonsson, T.; Sjoback, R. *J. Biol. Chem*. **1999**, *274*, 17379.
(34) Mao, C.; Sun, W.; Shen, Z.; Seeman, N. C. *Nature* **1999**, *397*, 144.
(35) Lorenz, M.; Hillisch, A.; Payet, D.; Buttinelli, M.; Travers, A.; Diekmann, S. *Biochemistry* **1999**, *38*, 12150.
(36) Vámosi, G.; Gohlke, C.; Clegg, R. M. *Biophys. J*. **1996**, *71*, 972.
(37) Edman, L.; Mets, Ü.; Rigler, R. *Proc. Natl. Acad. Sci. U.S.A.* **1996**, *93*, 6710.
(38) Wennmalm, S.; Edman, L.; Rigler, R. *Proc. Natl. Acad. Sci. U.S.A.* **1997**, *94*, 10641.
(39) Edman, L.; Wennmalm, S.; Tamsen, F.; Rigler, R. *Chem. Phys. Lett*. **1998**, *292*, 15.
(40) Wennmalm, S.; Edman, L.; Rigler, R. *Chem. Phys*. **1999**, *247*, 61.
(41) Osborne, M. A.; Balasubramanian, S.; Furey, W. S.; Klenerman, D. *J. Phys. Chem. B* **1998**, *102*, 3160.
(42) Clegg, R. M. In *Fluorescence Imaging Spectroscopy and Microscopy*; Wang, X. F., Herman, B., Eds.; John Wiley & Sons: New York, 1996; Chapter 7.
(43) Dale, R. E.; Eisinger, J. *Biopolymers* **1974**, *13*, 1573.
(44) Haas, E.; Katchalski-Katzir, E.; Steinberg, I. Z. *Biopolymers* **1978**, *17*, 11.
(45) Stryer, L. *Annu. Rev. Biochem.* **1978**, *47*, 819.
(46) Dovichi, N. J.; Chen, D. D. In *Single Molecule Optical Detection, Imaging and Spectroscopy*, Basche, T., Moerner, W. E., Orrit, M., Wild, U. P., Eds.; Wiley: New York, 1997; P223.
(47) Bustamante, C.; Marko, J. F.; Siggia, E. D.; Smith, S. *Science* **1994**, *265*, 1599.
(48) Smith, S. B.; Cui, Y.; Bustamante, C. *Science* **1996**, *271*, 795.
(49) Rivetti, C.; Walker, C.; Bustamante, C. *J. Mol. Biol*. **1998**, *280*, 41.
(50) Mills, J. B.; Vacano, E.; Hagerman, P. J. *J. Mol. Biol*. **1999**, *285*, 245.